Kinetics of Metal-Mediated One-Electron Oxidation of Guanine in Polymeric DNA and in Oligonucleotides Containing Trinucleotide Repeat Sequences

Ivana V. Yang and H. Holden Thorp*

Department of Chemistry, The University of North Carolina, Chapel Hill, North Carolina 27599-3290

Received June 6, 2000

The oxidation of guanines in DNA by Ru(III) is investigated by catalytic electrochemistry and stopped-flow spectrophotometry. The reactions of calf thymus DNA (20% guanine) and herring testes DNA (25% guanine) with $Ru(bpy)_3^{3+}$ (bpy = 2,2′-bipyridine) show biexponential decays in stopped-flow spectrophotometric experiments with the fast and slow components in 2:1 ratios and average rate constants in 880 mM NaCl of $\langle k \rangle = 18\ 700\ M^{-1}\ s^{-1}$ for calf thymus DNA and $\langle k \rangle = 24\ 600\ M^{-1}\ s^{-1}$ for herring testes DNA. The higher rate constant for the more guanine-rich DNA is possibly due to a higher density of electron-rich guanine multiplets. The observation of a biexponential decay is incorporated into digital simulations of the catalytic voltammograms observed for $Ru(bpy)_3^{2+}$ in the presence of DNA. For both DNAs, the rates observed by voltammetry are somewhat slower than those observed by stopped-flow spectrophotometry and the dependence of the rate constants on scan rate using the biexponential model is less pronounced than when only one decay is treated, supporting the notion that the scan rate dependence arises from the multiphasic decay. At low salt concentrations, where binding of the metal complex to DNA increases the effective catalytic rate constant, rates can be measured by stopped-flow spectrophotometry only with a less oxidizing complex, $Fe(bpy)_3^{3+/2+}$, which yields trends in the rate constants similar to those observed for the case of $Ru(bpy)_3^{3+/2+}$ at high ionic strength. Oligonucleotides based on the trinucleotide repeat sequences $(AGT)_n$ and $(GAA)_n$ produce significant catalytic currents, which are readily interpreted in terms of the guanine concentration and the secondary structure discerned from gel electrophoresis experiments. These experiments may provide a basis for sensing secondary structures and repeat numbers in biologically relevant DNAs.

Introduction

Electrochemistry offers an attractive approach to genetic analysis for a number of reasons that have been previously discussed.[1−16] A challenge in developing electrochemical methods for nucleic acid analysis is the identification of the appropriate redox-active moiety to analyze. For direct analysis, oxidation of the nucleic acid bases is the most facile; however, the potentials required for these reactions are high and generally near those where most electrodes oxidize water.[11,13] Other electrochemical approaches center on detection of exogenous redox labels that either interact specifically with double-stranded DNA[3−5,7−9,12,14−16] or are covalently attached to the target nucleic acid.[1,2,6,10]

We have described an electrochemical approach to nucleic acid analysis where DNA sequence and structure are probed by $Ru(bpy)_3^{2+}$-mediated oxidation of guanine nucleobases ($E_{1/2}$[Ru(III/II)] = 1.06 V and $E_{1/2}$[G(1+/0)] ∼1.1 V vs Ag/AgCl).[17−19] This method is based on the detection of current enhancement in the cyclic voltammogram of $Ru(bpy)_3^{2+}$ measured at indium tin oxide (ITO) electrodes in the presence of DNA (bpy = 2,2′-bipyridine). The large number of guanine bases present in polymeric DNA combined with the use of miniaturized electrodes may allow detection of small amounts of genomic DNA fragments. In fact, we recently reported detection of immobilized DNA on ITO electrodes at a density of only 44 amol/mm^2.[20] This method is attractive because the ITO electrodes do not oxidize water or guanine significantly at the potential where the $Ru(bpy)_3^{3+/2+}$ couple occurs and the rate constant for $Ru(bpy)_3^{3+}$-guanine electron transfer is ex-

(1) Caruana, D. J.; Heller, A. *J. Am. Chem. Soc.* **1999**, *121*, 769−774.
(2) Hartwich, G.; Caruana, D. J.; deLumley-Woodyear, T.; Wu, Y.; Campbell, C. N.; Heller, A. *J. Am. Chem. Soc.* **1999**, *121*, 10803−10812.
(3) Hashimoto, K.; Ito, K.; Ishimori, Y. *Anal. Chem.* **1994**, *66*, 3830−3833.
(4) Kelley, S. O.; Barton, J. K.; Jackson, N. M.; Hill, M. G. *Bioconjugate Chem.* **1997**, *8*, 31−37.
(5) Kelley, S. O.; Boon, E. M.; Barton, J. K.; Jackson, N. M.; Hill, M. G. *Nucleic Acids Res.* **1999**, *27*, 4830−4837.
(6) Korri-Youssoufi, H.; Garnier, F.; Srivastava, P.; Godillot, P.; Yassar, A. *J. Am. Chem. Soc.* **1997**, *119*, 7388−7389.
(7) Marrazza, G.; Chianella, I.; Mascini, M. *Biosens. Bioelectron.* **1999**, *14*, 43−51.
(8) Millan, K. M.; Mikkelsen, S. R. *Anal. Chem.* **1993**, *65*, 2317−2323.
(9) Millan, K. M.; Saraullo, A.; Mikkelsen, S. R. *Anal. Chem.* **1994**, *66*, 2943−2948.
(10) O'Connor, S. D.; Olsen, G. T.; Creager, S. E. *J. Electroanal. Chem. Interfacial Electrochem.* **1999**, *466*, 197−202.
(11) Palecek, E.; Fojta, M. *Anal. Chem.* **1994**, *66*, 1566−1571.
(12) Takenaka, S.; Yamashita, K.; Takagi, M.; Uto, Y.; Kondo, H. *Anal. Chem.* **2000**, *72*, 1334−1341.
(13) Wang, J.; Rivas, G.; Fernandes, J. R.; Paz, J. L. L.; Jiang, M.; Waymire, R. *Anal. Chim. Acta* **1998**, *375*, 197−203.
(14) Wang, J.; Fernandes, J. R.; Kubota, L. T. *Anal. Chem.* **1998**, *70*, 3699−3702.
(15) Xu, X.-H.; Yang, H. C.; Mallouk, T. E.; Bard, A. J. *J. Am. Chem. Soc.* **1994**, *116*, 8386-8387.
(16) Xu, X.-H.; Bard, A. J. *J. Am. Chem. Soc.* **1995**, *117*, 2627−2631.
(17) Johnston, D. H.; Thorp, H. H. *J. Phys. Chem.* **1996**, *100*, 13873−13843.
(18) Johnston, D. H.; Glasgow, K. C.; Thorp, H. H. *J. Am. Chem. Soc.* **1995**, *117*, 8933−8938.
(19) Steenken, S.; Jovanovic, S. V. *J. Am. Chem. Soc.* **1997**, *119*, 617−618.
(20) Armistead, P. M.; Thorp, H. H. *Anal. Chem.* **2000**, *72*, 3764−3770.

10.1021/ic000607g CCC: $19.00
Published on Web 09/29/2000

tremely large, approaching 10^6 M^{-1} s^{-1}.[21] Accordingly, large current enhancements are obtained for micromolar concentrations of $Ru(bpy)_3^{2+}$ even when the DNA concentration is less than that of the catalyst.[21]

We have utilized the cyclic voltammetry simulation program DigiSim[22] to analyze the catalytic mechanism and extract rate constants for guanine oxidation in different DNA environments.[17,18,21] A relatively simple mechanism can be used for the case at high ionic strength where binding of the metal complex to DNA can be neglected:

$$Ru(bpy)_3^{3+} + e^- \rightleftarrows Ru(bpy)_3^{2+} \quad (1)$$

$$Ru(bpy)_3^{3+} \rightleftarrows Ru(bpy)_3^{2+} \quad (2)$$

$$Ru(bpy)_3^{3+} + DNA \rightarrow Ru(bpy)_3^{2+} + DNA' \quad (3)$$

$$Ru(bpy)_3^{3+} + DNA' \rightarrow Ru(bpy)_3^{2+} + DNA'' \quad (4)$$

Here DNA′ is a DNA molecule where one electron has been removed from guanine and DNA″ is a DNA molecule where two electrons have been removed from guanine. The mechanism accounts for slow spontaneous conversion of the oxidized metal complex back to the reduced form (eq 2), which is known to occur at neutral pH.[23] The mechanism also provides for DNA overoxidation (eq 4), since many guanine oxidation products are more easily oxidized than guanine itself.[24] At high salt concentration, the rate constant for oxidation of guanine in calf thymus DNA (eq 3) is $\sim 1 \times 10^4$ M^{-1} s^{-1} according to cyclic voltammetry; this value has been confirmed independently by pulsed voltammetry, chronoamperometry, and stopped-flow spectrophotometry.[18]

At low ionic strength, electrostatic binding of the mediator to the nucleic acid increases the catalytic current enhancement and accelerates the rate of guanine oxidation by an order of magnitude. This binding equilibrium complicates the mechanism, however, because square schemes accounting for bound and free ruthenium must be added for each electron transfer.[17] In addition, chronoamperometry studies have shown that, at low salt concentrations, the reaction exhibits biphasic kinetics with rates that differ by roughly an order of magnitude.[21] The biphasic nature of the reaction is also apparent in the scan rate dependence of the rate constants obtained from cyclic voltammetry. We have shown that the Λ and Δ enantiomers of $Ru(bpy)_3^{2+}$ oxidize guanine with similar rates, eliminating the possibility that the biphasic kinetics are a result of the stereoisomerism of the metal complex.[21]

We now extend our studies to $Ru(bpy)_3^{2+}$-mediated oxidation of polymeric and oligomeric DNAs containing different numbers of guanines. The primary question we address is whether the scan rate dependence from cyclic voltammetry is apparent as biphasic kinetics in homogeneous reactions that do not involve a solid electrode. This question was investigated by performing parallel studies of the oxidations of polymeric and oligonucleotide DNAs by stopped-flow spectrophotometry and cyclic voltammetry. A consistent model has been developed for analyzing both kinds of kinetic data where the stopped-flow results can be used to guide the electrochemical analysis. We also address three additional questions. First, what is the effect of changing the density of guanine in each strand of DNA? Second, how do noncanonical DNA structures affect the electrochemical response and apparent rate constant? Finally, since samples such as calf thymus DNA contain many sequences and fragment lengths, what is the role of polydispersity in the DNA sample? These questions have been addressed by studying the reactions of genomic DNAs from calf thymus and herring testes, which have different percentages of guanine (20% and 25%, respectively).[25] In addition, we have studied monodisperse oligonucleotides consisting of triplet repeats that contain a single guanine; such sequences are relevant to the disease-causing trinucleotide expansions that occur in genomic DNAs.[26−28]

Experimental Section

Materials. Calf thymus and herring testes DNA samples were purchased from Sigma and sheared by repeated sonication and passage through a 22-gauge needle.[29] Synthetic oligonucleotides were purchased from the Nucleic Acid Core Facility at the Lineberger Comprehensive Cancer Center of The University of North Carolina at Chapel Hill and purified on Microcon YM-3 centrifugal filters (Millipore). Water was purified with a Milli-Q purification system (Millipore). Salts for buffer preparation were purchased from Mallinckrodt, and ligands and metal salts were purchased from Aldrich. Published procedures were used to prepare the metal complexes $[Ru(bpy)_3]Cl_3$, $[Fe(bpy)_3]Cl_3$,[30] and $[Os(bpy)_2(dppz)]Cl_2$,[31] (bpy = 2,2′-bipyridine, dppz = dipyridophenazine). Gel electrophoresis reagents (acrylamide, agarose, TBE buffer) were purchased from Bio-Rad. All solution concentrations were determined spectrophotometrically using a Hewlett-Packard HP 8452 diode array spectrophotometer and known extinction coefficients.[18,31,32] Extinction coefficients for oligonucleotides were calculated using the nearest-neighbor equation,[33] giving the concentration of nucleic acid in strand concentration. Solutions of double-stranded oligonucleotide were prepared by mixing 1:1.2 guanine-containing and complementary oligonucleotides in the desired buffers, heating at 90 °C for 5 min, and cooling the mixtures to room temperature over a period of 3 h.

Stopped-Flow Spectrophotometry. Kinetic experiments were carried out using an On Line Instrument Systems RSM-1000 stopped-flow spectrophotometer. The reactions were monitored spectrophotometrically from 350 to 580 nm for 2.0 s at 1000 scans/s for $Ru(bpy)_3^{3+}$ and for 5 min at 21 scans/s for $Fe(bpy)_3^{3+}$. Solutions were maintained at 25 ± 1 °C. $M(bpy)_3^{3+}$ (M = Ru, Fe) and DNA were dissolved in ~10 mM H_2SO_4 (pH 2) and pH 8 phosphate buffer, respectively, and these solutions were then mixed to give a solution that was 50 mM in sodium phosphate, pH 7, with or without 800 mM NaCl after mixing. Concentrations of $Ru(bpy)_3^{2+}$ and $Fe(bpy)_3^{3+}$ in each run were obtained from A_{min} and $A_{max}-A_{min}$ at 452 nm (ϵ = 14 600 M^{-1} cm^{-1}) and at 524 nm (ϵ = 8400 M^{-1} cm^{-1}), respectively. Second-order oxidation rate constants were determined by global analysis[34] of all the data using the SPECFIT software (Spectrum Software Associates, Chapel Hill, NC).

Voltammetry and Digital Simulation. Voltammograms were collected using an EG&G Princeton Applied Research 273A poten-

(21) Sistare, M. F.; Holmberg, R.; Thorp, H. H. *J. Phys. Chem. B* **1999**, *103*, 10718−10728.
(22) Rudolph, M.; Reddy, D. P.; Feldberg, S. W. *Anal. Chem.* **1994**, *66*, 595A−600A.
(23) Creutz, C.; Sutin, N. *Proc. Natl. Acad. Sci. U.S.A.* **1975**, *72*, 2858−2862.
(24) Burrows, C. J.; Muller, J. G. *Chem. Rev.* **1998**, *98*, 1109−1151.
(25) Sigma Technical Support, 1997.
(26) Paulson, H. L.; Fischbeck, K. H. *Annu. Rev. Neurosci.* **1996**, *19*, 79−107.
(27) Sutherland, G. R.; Richards, R. I. *Proc. Natl. Acad. Sci. U.S.A.* **1995**, *92*, 3636−3641.
(28) Wells, R. D. *J. Biol. Chem.* **1996**, *271*, 2875−2878.
(29) Chaires, J. B.; Dattagupta, N.; Crothers, D. M. *Biochemistry* **1982**, *21*, 3933−3940.
(30) DeSimone, R. E.; Drago, R. S. *J. Am. Chem. Soc.* **1970**, *92*, 2343−2352.
(31) Welch, T. W.; Corbett, A. H.; Thorp, H. H. *J. Phys. chem.* **1995**, *99*, 11757−11763.
(32) Sambrook, J.; Fritsch, E. F.; Maniatis, T. *Molecular cloning: a laboratory manual*; Cold Spring Harbor: Plainview, NY, 1989.
(33) *CRC Handbook of Biochemistry and Molecular Biology*,3rd ed.; Fasman, G. D., Ed.; CRC Press: Cleveland, OH, 1976; Section B, Vol. 1.
(34) Meader, M.; Zuberbuhler, A. D. *Anal. Chem.* **1990**, *62*, 2220−2224.

tiostat/galvanostat with a single-compartment cell[35] equipped with a tin-doped indium oxide (ITO) working electrode having a geometric area of 0.32 cm^2 (Delta Technologies), a Pt-wire auxiliary electrode, and a Ag/AgCl reference electrode (Cypress Sytems). ITO electrodes were cleaned as described previously,[36] and a freshly cleaned electrode was used for each experiment. Normal-pulse voltammograms were collected and simulated using the COOL software package according to a published procedure.[31] For cyclic voltammetry experiments, the electrode was conditioned by scanning in buffer between 0.0 and 1.3−1.4 V for seven cycles, followed by a background scan of buffer alone that was subtracted from subsequent scans. Cyclic voltammograms of 50 μM $Ru(bpy)_3^{2+}$ in the absence and the presence of DNA were collected for each electrode. Second-order rate constants for DNA oxidation by $Ru(bpy)_3^{2+}$ were determined by fitting of cyclic voltammetric data using the DigiSim 2.1 software package (Bioanalytical Systems). The complete fitting procedure and parameters used have been described elsewhere.[17,21] Diffusion coefficients of calf thymus and herring testes DNAs were obtained by normal-pulse voltammetry (see below), and those of synthetic oligonucleotides were calculated using the equation of Tirado and Garcia de la Torre.[37−39]

Gel Electrophoresis. Sizes of sheared DNA fragments were determined on a 0.9% agarose gel according to standard procedures.[32] $d(GAA)_n$ and $d(AGT)_n$ (n = 6 or 9) oligonucleotides were 5′-radiolabeled using T4 polynucleotide kinase (New England Biolabs) and 5′-[γ-^{32}P]dATP (Amersham).[32] Unreacted 5′-[γ-^{32}P]dATP was removed from the labeled oligonucleotide using a NucTrap column from Stratagene. Radiolabeled oligonucleotide (25−50 000 cpm) was added to a solution of cold oligonucleotide alone (25 μM) or cold oligonucleotide with 30 μM complementary $d(TTC)_9$ or $d(ACT)_9$ oligonucleotide in 50 mM sodium phosphate buffer with 800 mM NaCl. Oligonucleotides were annealed, loaded on a 20% nondenaturing polyacrylamide gel, and electrophoresed at 4 °C and 200 V for 8 h. The gel was exposed on a phosphorimager screen overnight and scanned using a Storm 840 system (Molecular Dynamics).

Results and Discussion

Polymeric DNA: High Salt. (a) Stopped-Flow Spectrophotometry. Our experimental strategy was to study the kinetics of the homogeneous DNA oxidation by stopped-flow spectrophotometry and then to use the results of these experiments in modifying the electrochemical model. Initial investigations centered on reactions at high sodium ion concentration where binding of $Ru(bpy)_3^{3+/2+}$ to DNA can be neglected.[18] As expected from the scan rate dependence of the cyclic voltammetry,[21] single-wavelength kinetic traces exhibited biphasic kinetics and fit best to double-exponential functions (i.e., $A_1 \exp(-k_1 t) + A_2 \exp(-k_2 t)$). The ratios of the intensities of the fast and slow components (i.e., A_1:A_2) for these curves were ∼2:1. These ratios were used in subsequent global fitting of the data at multiple wavelengths (350−600 nm), which was performed in SPECFIT according to a kinetic model consisting of two parallel oxidations by noninterconvertible Ru^{3+} populations:

$$Ru1^{3+} + DNA \xrightarrow{k_1} Ru^{2+} + DNA' \quad (5)$$

$$Ru2^{3+} + DNA \xrightarrow{k_2} Ru^{2+} + DNA' \quad (6)$$

where $Ru1^{3+}$ and $Ru2^{3+}$ indicate species of Ru(III) and the ratio $[Ru1^{3+}]/[Ru2^{3+}]$ was constrained to a value of 2. A representative kinetic trace at 452 nm with the global analysis fit is shown in Figure 1A. The calculated absorption spectra shown in Figure 1B agree well with the known spectra of $Ru(bpy)_3^{2+}$ and $Ru(bpy)_3^{3+}$.[40] From inspection of the early-time points in Figure 1A, there appears to be another minor contribution from an even faster process not accounted for by the two species in eqs 5 and 6. We have chosen not to analyze this minor process rather than to add another set of parameters, although triexponential processes in DNA have been described.[41,42]

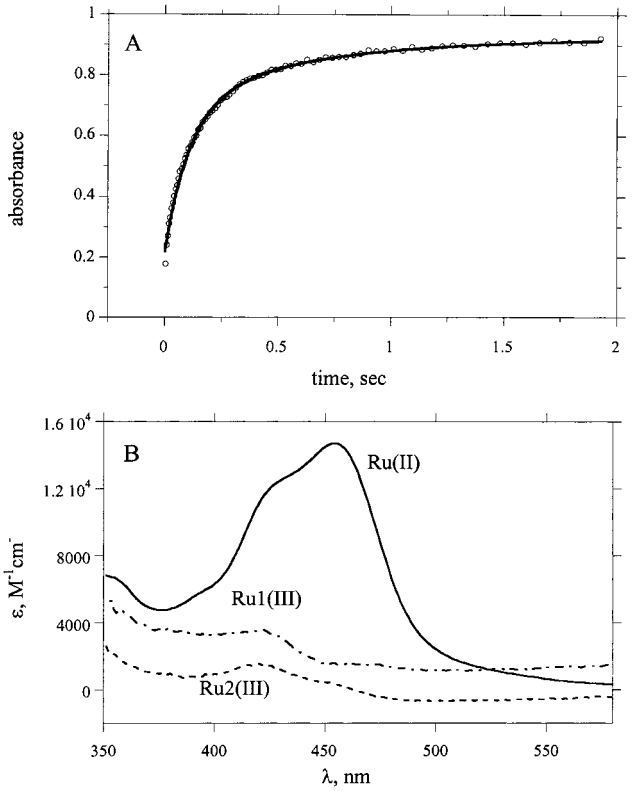

Figure 1. (A) Absorbance at 452 nm versus time for the oxidation of herring testes DNA by $Ru(bpy)_3^{3+}$ at high ionic strength. The solid line shows the calculated time dependence from global analysis. (B) Calculated spectra of Ru^{2+}, $Ru1^{3+}$, and $Ru2^{3+}$ determined in the global analysis.

Second-order rate constants in terms of guanine concentration determined by global analysis of the stopped-flow data (as in Figure 1) are summarized in Table 1. A number of important points are apparent. First, the rate constant for the faster component of the reaction of $Ru(bpy)_3^{3+}$ with calf thymus DNA is in excellent agreement with the value we previously reported for this reaction obtained from stopped-flow spectrophotometry with fitting to a single population ($24 \times 10^3\ M^{-1}\ s^{-1}$).[18] Second, the rate constant for the slower component of the reaction of $Ru(bpy)_3^{3+}$ with calf thymus DNA agrees well with the rate constant obtained by chronoamperometry ($3.5 \times 10^3\ M^{-1}\ s^{-1}$).[21] Third, the more abundant $Ru1^{3+}$ population oxidizes guanines in double-stranded DNA almost an order of magnitude faster than $Ru2^{3+}$. This ratio of rates is similar to that obtained for the two observed components in oxidation of calf thymus DNA from recent chronoamperometry experiments at low ionic strength.[21]

(35) Willit, J. L.; Bowden, E. F. *J. Phys. Chem.* **1990**, *94*, 8241−8246.
(36) Welch, T. W.; Thorp, H. H. *J. Phys. Chem.* **1996**, *100*, 13829−13836.
(37) Tirado, M. M.; Garcia de la Torre, J. *J. Chem. Phys.* **1980**, *73*, 1986−1993.
(38) Tirado, M. M.; Garcia de la Torre, J. *J. Chem. Phys.* **1979**, *71*, 2581−2587.
(39) Garcia de la Torre, J.; Lopez Martinez, M. C.; Tirado, M. M. *Biopolymers* **1984**, *23*, 611−615.
(40) Kalyanasundaram, K. *Coord. Chem. Rev.* **1982**, *46*, 159.
(41) Netzel, T. L.; Zhao, M.; Nafisi, K.; Headrick, J.; Sigman, M. S.; Eaton, B. E. *J. Am. Chem. Soc.* **1995**, *117*, 9119−9128.
(42) Netzel, T. L.; Nafisi, K.; Zhoa, M. *J. Phys. Chem.* **1995**, *99*, 17936−17947.

Table 1. Second-Order Rate Constants from Stopped-Flow Spectrophotmetry for Guanine Oxidation by $Ru(bpy)_3^{3+}$

DNA[a]	M	% guanine	[NaCl], mM	k_1,[b] M^{-1} s^{-1}	k_2,[b] M^{-1} s^{-1}	$\langle k \rangle$, M^{-1} s^{-1}
calf thymus	Ru	20	800	26 400 ± 700	3300 ± 600	18 700[c]
	Fe		0	480 ± 40	45 ± 9	260[d]
herring testes	Ru	25	800	34 100 ± 800	5500 ± 300	24 600[c]
	Fe		0	720 ± 60	86 ± 4	400[d]
$(GAA)_9(TTC)_9$	Ru	16	800	31 000 ± 600	3900 ± 200	17 500[d]
	Fe		0	240 ± 60	26 ± 4	130[d]

[a] [G] = [nucleotide phosphate DNA]/5 for calf thymus DNA and nucleotide phosphate DNA/4 for herring testes DNA. [G] = 9 [strand DNA] for the $(GAA)_9(TTC)_9$ oligonucleotide. [b] Each reported value is a mean (±1 standard deviation) of four to six rate constants at different DNA and metal concentrations. [c] $\langle k \rangle = (2k_1 + k_2)/3$. [d] $\langle k \rangle = (k_1 + k_2)/2$.

A final point from Table 1 is that both k_1 and k_2 are higher for herring testes DNA than for calf thymus DNA. The rate constants are given in terms of moles of guanine, so the higher fraction of guanine in herring testes DNA is already accounted for in the model. A possible explanation for this increase is a higher number of GG steps in herring testes DNA. The 5′ guanine in GG sequences is more easily oxidized than guanines that are 5′ to other bases due to more favorable stacking interactions with the adjacent guanine.[43−45] As shown previously with defined sequences, larger numbers of GG steps in the sequence increase the apparent rate constant when normalized to the total number of guanines.[45] For comparison, the weighted average rate constants, $\langle k \rangle = (2k_1 + k_2)/3$, are also given in Table 1.

In addition to the two-population model in eqs 5 and 6, two alternative kinetic models were tested. The first involved overoxidation of guanine instead of a parallel oxidation process, since we have shown that overoxidation steps improve the fitting of cyclic voltammetry results and are easily envisioned on the basis of the chemistry of guanine oxidation.[17,21,24] We also examined the possibility of nonproductive Ru^{3+} reduction (i.e., eq 3) accounting for the second exponential in the kinetic trace, since $Ru(bpy)_3^{3+}$ is known to convert independently to the 2+ form at neutral pH.[23] The data were not fit well by either mechanism; these two steps are probably too slow to contribute to the decay on the stopped-flow time scale.

(b) Cyclic Voltammetry. Having established that the homogeneous reaction proceeds with biphasic kinetics and a 2:1 ratio of subpopulations, we next sought to use this information in the electrochemical simulations. However, we first required values for the diffusion coefficients of the biopolymers. These were determined by electrochemistry of a nonoxidizing probe molecule with high DNA-binding affinity, as previously described.[31] Calf thymus DNA and herring testes DNA were sheared to generate shorter and more homogeneous DNA samples. Sizes of these sheared DNA fragments were estimated independently by gel electrophoresis to be between 1000 and 3000 base pairs (bp) for calf thymus (compared to >12 000 bp for unsheared) and between 500 and 1000 bp for herring testes (compared to 700−3000 bp for unsheared). Apparent diffusion coefficients of the fragments were determined using normal-pulse voltammetry with the $Os(bpy)_2(dppz)^{2+}$ intercalator (dppz = dipyridophenazine).[31] This technique provides diffusion coefficients for DNA molecules with an accuracy comparable to that of light-scattering experiments and theoretical calculations.[31,37−39,46,47] Analysis of normal-pulse voltammograms of $Os(bpy)_2(dppz)^{2+}$ in the presence of sheared calf thymus and herring testes DNAs gave diffusion coefficients of 1.8×10^{-7} and 2.1×10^{-7} cm^2/s, respectively.

With the DNA diffusion coefficients known, the mechanism established by stopped-flow spectrophotometry could then be used as the basis for simulating the electrochemical data. Cyclic voltammograms of $Ru(bpy)_3^{2+}$ in the presence of 1.0, 1.5, and 2.0 mM calf thymus or herring testes DNA at a range of scan rates (10−250 mV/s) were collected. High concentrations and relatively slow scan rates were necessary to observe different amounts of catalytic current enhancement for calf thymus and herring testes DNAs at the same nucleotide concentration. The mechanism employed in the fitting of cyclic voltammograms was similar to the mechanism we have previously reported (eqs 1−4),[17] except that two noninterconvertible ruthenium populations were used for the initial electron transfer, as observed in the stopped-flow studies. The ratio $[Ru1^{3+}]/[Ru2^{3+}] = 2$ was taken from the fitting of the stopped-flow data. Two further oxidations by the more reactive $Ru1^{3+}$ population were required to fit the data, which are in contrast to the stopped-flow spectrophotometry data, where no overoxidation reactions are apparent. The complete mechanism entered into DigiSim simulation program is shown in eqs 7−14, where DNA‴ is DNA that has been oxidized by three electrons.

$$Ru1^{2+} \rightleftarrows Ru1^{3+} + e^- \quad (7)$$

$$Ru2^{2+} \rightleftarrows Ru2^{3+} + e^- \quad (8)$$

$$Ru1^{3+} \rightleftarrows Ru1^{2+} \quad (9)$$

$$Ru2^{3+} \rightleftarrows Ru2^{2+} \quad (10)$$

$$Ru1^{3+} + DNA \xrightarrow{k_1} Ru1^{2+} + DNA' \quad (11)$$

$$Ru1^{3+} + DNA' \xrightarrow{k_1'} Ru1^{2+} + DNA'' \quad (12)$$

$$Ru1^{3+} + DNA'' \xrightarrow{k_1''} Ru1^{2+} + DNA''' \quad (13)$$

$$Ru2^{3+} + DNA \xrightarrow{k_2} Ru2^{2+} + DNA' \quad (14)$$

A representative set of cyclic voltammograms overlaid with DigiSim fits is shown in Figure 2A. The rate constants obtained from the simulations did not show a systematic dependence on the DNA concentration and are given in Table 2 as averages from three concentrations at 10 and 250 mV/s for both calf thymus and herring testes DNAs. The values of k_1 agree well with the rate constant we have previously determined for oxidation of guanine in calf thymus DNA at high ionic strength by cyclic voltammetry ($\sim 1 \times 10^4$ $M^{-1}s^{-1}$),[18] where the data were fit to only one population. The ratio of rates for the initial electron transfer in the faster and the slower components varied with the scan rate between 10 and 60, with the lower limit being

(43) Saito, I.; Nakamura, T.; Nakatani, K.; Yoshioka, Y.; Yamaguchi, K.; Sugiyama, H. *J. Am. Chem. Soc.* **1998**, *120*, 12686−12687.
(44) Sugiyama, H.; Saito, I. *J. Am. Chem. Soc.* **1996**, *118*, 7063−7068.
(45) Sistare, M. F.; Codden, S. J.; Heimlich, G.; Thorp, H. H. *J. Am. Chem. Soc.* **2000**, *122*, 4742−4749.
(46) Eimer, W.; Pecora, R. *J. Chem. Phys.* **1991**, *94*, 2324−2329.
(47) Goinga, H. T.; Pecora, R. *Macromolecules* **1991**, *24*, 6128−6138.

Table 2. Second-Order Rate Constants from Electrochemistry for Guanine Oxidation by $Ru(bpy)_3^{3+}$ in Polymeric DNA at High Salt Concentrations

DNA[a]	v, mV/s	10^3k_1,[b] M^{-1} s^{-1}	$10^3k_1'$,[b] M^{-1} s^{-1}	$10^3k_1''$,[b] M^{-1} s^{-1}	10^3k_2,[b] M^{-1} s^{-1}	$\langle k\rangle$,[c] M^{-1} s^{-1}
calf	10	6.2 ± 1.1	5.9 ± 3.0	6.0 ± 3.5	0.59 ± 0.38	4 300
thymus	250	17 ± 3.1	11 ± 1.6	0	0.75 ± 0.30	11 600
herring	10	6.8 ± 1.4	5.1 ± 0.90	5.3 ± 1.4	0.39 ± 0.26	4 700
testes	250	21.4 ± 5.1	12 ± 2.5	0	0.89 ± 0.30	14 600

[a] [G] = [nucleotide phosphate DNA]/5 for calf thymus and [nucleotide phosphate DNA]/4 for herring testes DNA. [b] Each reported value is a mean ($\pm$1 standard deviation) of three rate constants (1.0, 1.5, and 2.0 mM nucleotide phosphate DNA). [c] $\langle k\rangle = (2k_1 + k_2)/3$.

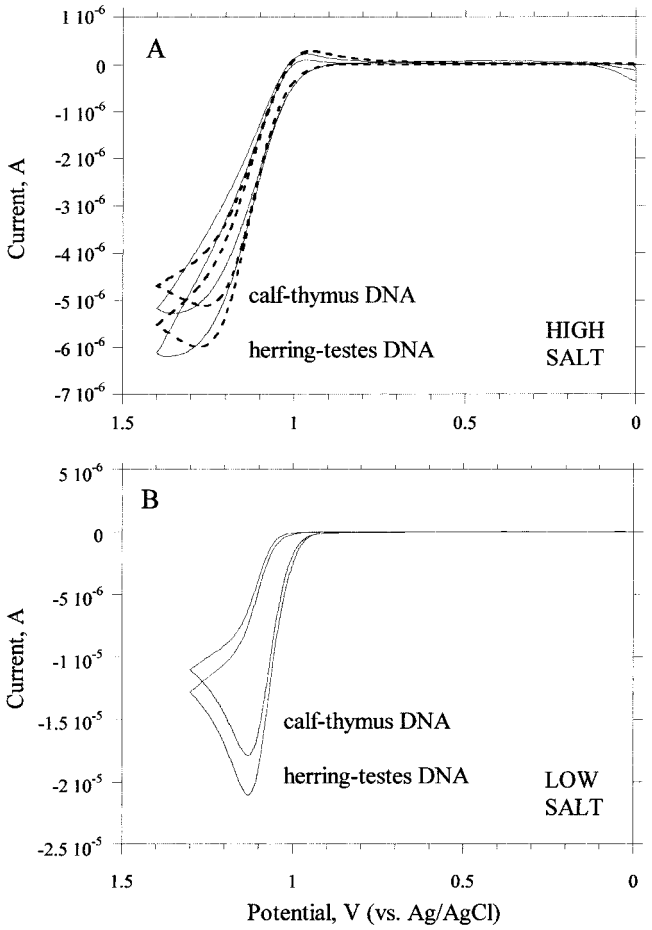

Figure 2. Cyclic voltammograms (solid) and digital simulations (dashed; calculated using eqs 7−14) for 50 μM $Ru(bpy)_3^{2+}$ with 2.0 mM calf thymus or herring testes DNA in (A) 50 mM sodium phosphate, pH 7, with 800 mM NaCl and (B) 50 mM sodium phosphate, pH 7, at 50 mV/s.

in good agreement with the ratio of the two components determined by chronoamperometry.[21]

Rate constants for both the faster and the slower component are lower than those obtained from stopped-flow spectrophotometry. We suspect that this relationship is a result of the longer time scale in the cyclic voltammetric experiment and the subsequent need for the addition of overoxidation steps, which provide an additional pathway for Ru(III) reduction not needed in the stopped-flow model. Accordingly, fitting of cyclic voltammograms collected at higher scan rates, i.e., shorter reaction times, required fewer overoxidation steps and gave k_1 values that approach the values obtained in the stopped-flow experiment (Table 2). However, the relative amount of catalytic current enhancement decreases with increasing scan rate because of the lower number of catalytic cycles at shorter reaction times, which leads to a larger error. At present, we are unsure as to whether the overoxidation steps are required because the longer time scale allows for additional reactions or because the simulation model is in some way limited. Parallel investigation of oxidation products and reaction kinetics should allow us to clarify this point in the future.

As discussed above, our primary goal was to determine whether the inclusion of multiple rate constants in the fitting of the electrochemical data reduces the dependence of the simulated rate constants on the scan rate observed when only one population is used. In Table 2, the rate constants obtained from the simulation of cyclic voltammograms with two populations of Ru(III) do show a modest scan rate dependence: the values of k_1 and k_1' increase with an increase in scan rate and the value of k_1'' becomes negligible at 250 mV/s. The values of k_2 do not change in a systematic fashion over the studied range of scan rates. Although the rate constants in Table 2 still show an experimentally significant scan rate dependence, the variation is much less pronounced than when only one population is used in the fit. In Table 2, the value of k_1 changes by a factor of 2 from 10 to 250 mV/s, which is much smaller than the scan rate dependence of the rate constant when only one ruthenium population is entered in the mechanism. In the latter case, the apparent rate changes by an order of magnitude on going from 25 to 250 mV/s.[21] Thus, use of two ruthenium populations reduces the scan rate dependence previously observed by digital simulation, supporting the proposal that biphasic kinetics in the guanine−Ru(III) electron transfer are responsible for the scan rate dependence.

Polymeric DNA: Low Salt. (a) Stopped-Flow Spectrophotometry. Studies on calf thymus and herring testes DNA were performed at low ionic strength to examine the effect of ruthenium binding to the DNA on the kinetics of guanine oxidation in the two polymers containing different amounts of guanine. Binding of $Ru(bpy)_3^{3+}$ to DNA in the absence of additional NaCl renders the rate of guanine oxidation approximately an order of magnitude faster than at high ionic strength,[17] making it difficult to study by stopped-flow spectrophotometry. To follow the faster reaction at low ionic strength, we decided to employ $Fe(bpy)_3^{3+}$, which is a close structural analogue of $Ru(bpy)_3^{3+}$ but has a lower redox potential ($E_{1/2}$ [Fe(III/II)] = 0.85 V), slowing the rate of guanine oxidation considerably.[18] The reaction was monitored at 524 nm in the same manner as the reaction of DNA with ruthenium at high ionic strength. SPECFIT analysis was also performed analogously to that for the ruthenium case, using the same mechanism (eq 5 and 6). The ratio of two iron populations was established by fitting of a double exponential to single-wavelength data and gave a ratio of $[Fe1^{3+}]/[Fe2^{3+}] = 1$, which differs from the 2:1 ratio of two ruthenium populations at high ionic strength. The difference in the ratios of the faster and the slower components is probably not significant. Second-order rate constants in terms of guanine concentrations for calf thymus and herring testes DNAs at various DNA concentrations are summarized in Table 1. The ratio of rate constants for the faster and slower component is similar to the ratio of the two components at high ionic strength, but the difference in rates of guanine oxidation in calf

thymus and herring testes DNAs is much more pronounced when binding of the metal complex is occurring, giving nearly a factor of 2 difference between herring testes and calf thymus DNAs. This difference could be due to an even more greatly enhanced reactivity of GG steps at low ionic strength compared to high ionic strength.

(b) Cyclic Voltammetry. Electrochemical studies on polymeric DNA substrates were also performed under conditions where metal complex binding to the polyanion must be considered. Cyclic voltammograms of $Ru(bpy)_3^{2+}$ at low ionic strength in the presence of 1.0, 1.5, and 2.0 mM calf thymus or herring testes DNA at 25 and 50 mV/s were collected; representative data are shown in Figure 2B. While the amount of current is much higher than that in the high ionic strength case, the binding of ruthenium to DNA does not enhance the relative difference in the amount of current enhancement in the presence of different amounts of guanine. This result demonstrates that small differences in the guanine content (20% vs 25%) can be detected in our system regardless of the ionic strength. We were not able to extract rate information from the cyclic voltammograms because the mechanism that accounts for both the ruthenium binding and the presence of the faster and the slower components has too many parameters, which were therefore not well determined.

Oligonucleotides. (a) Stopped-Flow Spectrophotometry—High Salt. Stopped-flow spectrophotometric studies with $Ru(bpy)_3^{3+}$ at high ionic strength were extended to smaller DNA molecules, namely, synthetic oligonucleotides containing trinucleotide repeat sequences. We chose to investigate the trinucleotide repeat effect in oligonucleotides based on $(GAA)_n$, which is expanded in the genomes of Friederich's ataxia patients.[26−28] This motif was chosen over other physiologically relevant sequences because of the lack of guanines in the complementary strand, which makes possible direct comparison the data for single- and double-stranded oligonucleotide in subsequent voltammetry experiments. The rate constants for oxidation of guanine in the double-stranded $(GAA)_9(TTC)_9$ oligonucleotide were extracted from stopped-flow data in the same manner as that used for the case of polymeric DNA molecules and are shown in Table 1. The most important observation is the biphasic nature of the electron-transfer reaction, with the ratio of two Ru^{3+} populations of 1:1. The biphasic kinetics of the reaction with oligonucleotides as the substrate suggests that polydispersity and sequence heterogeneity of DNA molecules are not the origin of the biphasic kinetics since synthetic oligonucleotides are all of the same length and their hybrids are too short to have unusual secondary structures. Rate constants for guanine oxidation are nearly identical in double-stranded oligonucleotides and in polymeric DNA samples (Table 1), which is reasonable since calf thymus and herring testes DNAs are almost completely double-stranded. The ratio of the faster and the slower component also remains constant regardless of the DNA sample. Thus, potential polydispersity in polymeric DNA samples does not appear to affect the rate of electron transfer.

(b) Cyclic Voltammetry—High Salt. Guanine oxidation in oligonucleotides containing triplet repeats was also investigated by cyclic voltammetry. Two trinucleotide repeat sequences were examined: $(GAA)_n$ and $(AGT)_n$, where $n = 6$ or 9. The $(AGT)_n$ repeat was included to study the effect of the base 3′ to the guanine, since the GA step in the $(GAA)_n$ repeat may be more reactive than the GT step in the $(AGT)_n$ repeat due to differential stacking of two purines compared to a purine and a pyrimidine.[43]

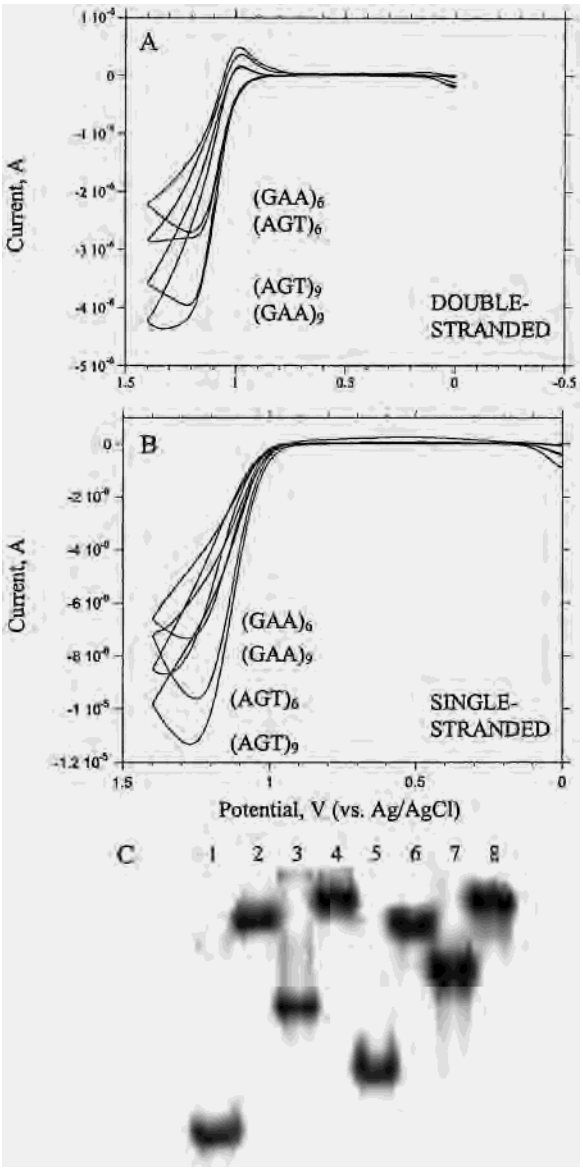

Figure 3. (A, B) Cyclic voltammograms of 50 μM $Ru(bpy)_3^{2+}$ with 25 μM double-stranded (ds) (A) and single-stranded (ss) (B) oligonucleotides in 50 mM sodium phosphate, pH 7, with 800 mM NaCl at 25 mV/s. (C) Nondenaturing polyacrylamide gel of $(GAA)_n$ and $(AGT)_n$ oligonucleotides visualized by phosphorimagery. Lanes: 1, ss $(GAA)_6$; 2, ds $(GAA)_6$; 3, ss $(GAA)_9$; 4, ds $(GAA)_9$; 5, ss $(AGT)_6$; 6, ds $(AGT)_6$; 7, ss $(AGT)_9$; 8, ds $(AGT)_9$.

Representative sets of cyclic voltammograms are shown in Figure 3A,B. Oligonucleotides containing six and nine triplet repeats are easily distinguished when single- or double-stranded. More catalytic current is observed for single-stranded oligonucleotides because of the higher solvent accessibility of single-stranded guanines compared to guanines inside the double helix.[18] Double-stranded $(GAA)_n$ and $(AGT)_n$ oligonucleotides show the same amount of current enhancement within experimental error, whereas single-stranded $(AGT)_n$ oligonucleotides produce more current than $(GAA)_n$ oligonucleotides. We suspected that this difference may be due to the presence of noncanonical secondary structures in $(GAA)_n$ oligonucleotides imposed by the ability of guanine and adenine to form Hoogsteen base pairs.[48] Nondenaturing gel electrophoresis under conditions identical to those in our electrochemical experiments

(48) *Nucleic Acids in Chemistry and Biology*; 2nd ed.; Blackburn, G. M., Gait, M. J., Eds.; Oxford University Press: New York, 1996.

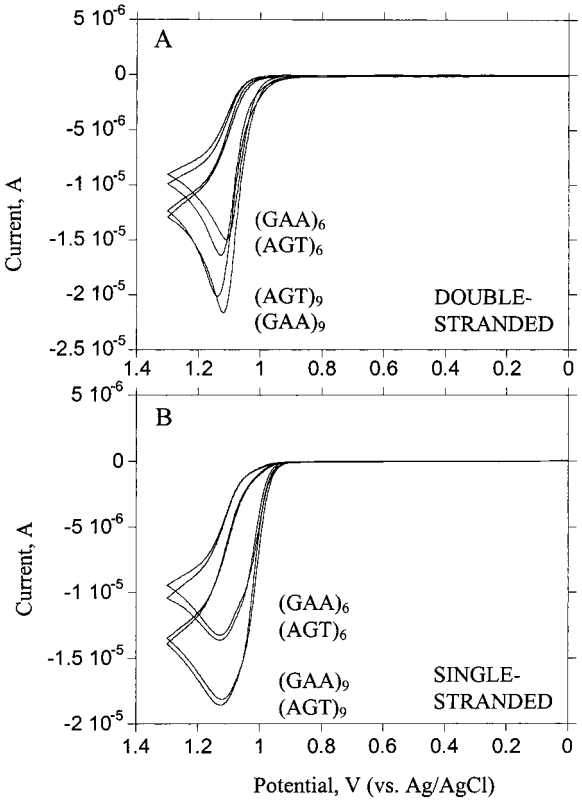

Figure 4. Cyclic voltammograms of 50 μM $Ru(bpy)_3^{2+}$ with 25 μM double-stranded (A) and single-stranded (B) oligonucleotides in 50 mM sodium phosphate, pH 7, at 25 mV/s.

(25 μM oligonucleotide in 50 mM sodium phosphate with 800 mM added sodium chloride; Figure 3C) supports this hypothesis, since the single-stranded forms of this oligonucleotide (lanes 1 and 3) migrate much faster than the single-stranded forms of the $(AGT)_n$ sequence (lanes 5 and 7). All of the annealed samples migrate as expected for the duplex forms. The results in Figure 3 provide a satisfying demonstration of how the electrochemistry can indicate changes in structure that can then be confirmed by traditional biochemical techniques.

(c) Cyclic Voltammetry—Low Salt. Cyclic voltammograms of $Ru(bpy)_3^{2+}$ in the presence of 25 μM single- and double-stranded $(GAA)_6$, $(GAA)_9$, $(AGT)_6$, and $(AGT)_9$ oligonucleotides at low ionic strength are shown in Figure 4. While the absolute amount of observed current is higher than that observed at high ionic strength (Figure 3), the relative difference between six and nine repeats remains the same both in double- (Figure 4A) and in single-stranded (Figure 4B) oligonucleotides. This situation is analogous to the comparison of calf thymus and herring testes DNAs at low and high ionic strengths and indicates that binding of the metal complex to DNA increases the overall signal but neither improves nor decreases the sensitivity for distinguishing different amounts of guanine. In contrast to the high ionic strength case, single-stranded $(GAA)_n$ and $(AGT)_n$ oligonucleotides show the same amount of current enhancement possibly because the noncanonical secondary structures in $(GAA)_n$ repeats (Figure 3C) form only at high sodium ion concentration.

A striking feature in Figure 4 compared to the voltammograms collected at high ionic strength is the similar currents observed for double- (Figure 4A) and single-stranded (Figure 4B) DNAs. In Figure 3 and in many other experiments performed at high salt concentration, we have observed much higher reactivity of single-stranded and mismatched guanines due to higher solvent accessibility.[18,49] Tighter binding of the metal cation to the double helix enhances the reactivity of double-stranded oligonucleotides; however, the guanines of single-stranded oligonucleotides are more solvent accessible and therefore more reactive. These effects are apparently contradictory; thus, the difference in absolute current for double- and single-stranded DNAs is small at low salt concentration. The voltammograms do differ in shape, where voltammograms of single-stranded DNA are much wider and voltammograms of double-stranded DNA have much sharper peaks.

(d) Distinguishing Repeat Numbers. In the final set of experiments, we examined the reactivity of oligonucleotides containing $(GAA)_n$ ($n = 5-9$) trinucleotide repeats. Here our goal was to determine whether the catalytic current was sufficient to distinguish addition of a single repeat to the sequence. To combine the advantages of better sensitivity at lower ionic strength and a simpler mechanism at high ionic strength, an intermediate ionic strength regime (50 mM sodium phosphate with 400 mM sodium chloride) was chosen. Cyclic voltammograms of 25 μM single- and double-stranded oligonucleotides at 25 mV/s are shown in Figure 5A,B, and plots of peak current vs number of repeats, *n*, are shown in Figure 5C. The peak current increases linearly with the number of repeats in both single- and double-stranded $(GAA)_n$ oligonucleotides. More current enhancement is observed in the case of single-stranded oligonucleotides, suggesting that the unbound ruthenium dominates at this ionic strength. However, the amount of current enhancement for $(GAA)_6$ and $(GAA)_9$ oligonucleotides is higher and the difference between single- and double-stranded DNAs is less pronounced when compared to those at high ionic strength (Figure 2), which implies that binding of ruthenium to DNA is detectable.

Conclusions

Biphasic Kinetics. The electron-transfer reaction of $M(bpy)_3^{3+}$ (M = Ru, Fe) with guanine nucleobases exhibits biphasic kinetics both in DNA polymers of heterogeneous sequences and in trinucleotide-repeat oligonucleotides at both high and low ionic strengths. This suggests that conformation, polydispersity, and sequence heterogeneity are not the origin of the two populations. Simple binding of the metal complex is likely not the source of the two populations either, since the two populations are present even when binding of the metal complex is negligible, i.e., at high Na^+ concentrations. We believe that the biphasic kinetics result simply from inclusion of guanine in a macromolecule (even in small oligonucleotides), which is supported by many observations of biphasic reaction kinetics for similar reactions.[50−53] As has been discussed elsewhere,[50−53] the two species likely result from different binding geometries that undergo a reaction (in this case electron transfer) that is fast compared to the diffusive interconversion of the two species.

Scan Rate Dependence. The scan rate dependence of the rate constants obtained from cyclic voltammetry is greatly diminished when the voltammograms are fit to the two-population model (Table 2) instead of the mechanism with only

(49) Ropp, P. A.; Thorp, H. H. *Chem. Biol.* **1999**, *6*, 599−605.
(50) Arkin, M. R.; Stemp, E. D. A.; Holmlin, R. E.; Barton, J. K.; Hormann, A.; Olson, E. J. C.; Barbara, P. F. *Science* **1996**, *273*, 475−480.
(51) Arkin, M. R.; Stemp, E. D. A.; Turro, C.; Turro, N. J.; Barton, J. K. *J. Am. Chem. Soc.* **1996**, *118*, 2267−2274.
(52) Barton, J. K.; Kumar, C. V.; Turro, N. J. *J. Am. Chem. Soc.* **1986**, *108*, 6391−6393.
(53) Kumar, C. V.; Barton, J. K.; Turro, N. J. *J. Am. Chem. Soc.* **1985**, *107*, 5518−5523.

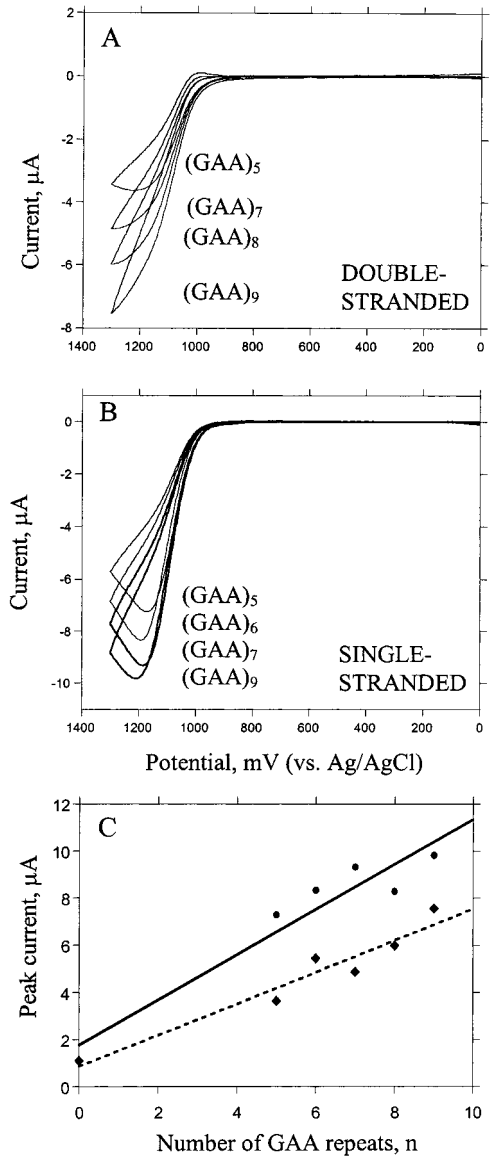

Figure 5. (A, B) Cyclic voltammograms of 50 μM $Ru(bpy)_3^{2+}$ with 25 μM double-stranded (A) and single-stranded (B) oligonucleotides in 50 mM sodium phosphate, pH 7, with 400 mM NaCl at 25 mV/s. (C) Plots of peak currents taken from voltammograms for double-stranded (◆) and single-stranded (●) oligonuclotides vs the number of GAA repeats, *n*. Solid and dashed lines are best linear fits of the data; $R = 0.96$.

one population used previously.[17,45] The apparent rate constants obtained from fits to the one-population model are therefore an average of the rate constants for two phases of the reaction with the relative contributions of the two phases varying with the scan rate. Thus, inclusion of the two populations in the model reduces the effect on the apparent rate constant of sampling a fraction of the reaction course at any given scan rate.

Effect of Guanine Density. Heterogeneous-sequence DNA polymers that differ in their guanine contents by only ~5% are easily distinguished by the current observed in cyclic voltammetry in both high and low ionic strength regimes. This effect is due in part to the increased guanine concentration, which increases the observed current. However, the change in absolute guanine concentration is accounted for in the modeled rate constants, which are given in terms of moles of guanine. Therefore, the polymers with higher guanine content are intrinsically more reactive than those with less. This effect may arise from a higher number of electron-rich GG doublets, which are 12 times more reactive than an isolated guanine.[45] Alternatively, the higher numbers of guanines may provide greater intrinsic reactivity due to an increase in the frequency of collisions that lead to electron-transfer. We have discussed these issues in detail elsewhere and examined these effects in oligonucleotides of known sequences.[21,45] Because the sequences present in calf thymus and herring testes DNAs are heterogeneous, this issue cannot be resolved with certainty.

Guanine-containing trinucleotide repeat sequences of different lengths are readily differentiated at high, low, and intermediate ionic strengths. The observed current enhancement increases linearly with the number of repeats at intermediate ionic strength. This is of special significance because it should allow for future detection of trinucleotide repeat expansion in clinical samples from patients with neurodegenerative disorders such as fragile X syndrome, Friedrich's ataxia, and myotonic dystrophy.[26−28]

Secondary-Structure Dependence. Single-stranded oligonucleotides are much more reactive than their double-stranded counterparts under high ionic strength conditions as a result of higher solvent accessibility of guanine nucleobases. This is not the case in the low-salt regime, where the more pronounced solvent accessibility of single-stranded guanines is counteracted by an enhanced affinity of the positively charged metal complex for the more negatively charged double-stranded DNA, leading to comparable reactivities of single- and double-stranded sequences. Noncanonical secondary structures of $(GAA)_n$ are apparent in the electrochemistry and are verified independently by native gel electrophoresis. These observations demonstrate that detection of guanine secondary structures is best performed at high ionic strength, while simple quantitation of guanine concentrations is best performed at low ionic strength, where different secondary structures exhibit similar rate constants.

Acknowledgment. The U.S. Army Medical Research and Materiel Command under contract DAMD17-98-1-8224 supported this work along with Xanthon, Inc. We thank Stephanie Weatherly, Brian Farrer, Carole Golden, and Veronika Szalai for helpful discussions.

IC000607G